Supplemental Materials

Molecular Biology of the Cell

Wirshing and Cram

Supplemental Materials

Molecular Biology of the Cell

Wirshing and Cram

Supplemental Figure Legends

Supplemental Figure1: GFP labeled nonmuscle myosin II (*nmy-1*) is functional and rescues ovulation defects of *nmy-1* null animals. Animals homozygous for the *nmy-1* null allele, *nmy-1(sb115),*show some elongation defects during development but due to the complimentary activity of *nmy-2* are able to mature to adulthood (Piekny 2003). However, *nmy-2* is not expressed in the spermatheca, and *nmy-1(sb115)* animals have severe ovulation defects. To determine if GFP::NMY-1 is functional, we tested if spermatheca specific expression of GFP::NMY-1 is sufficient to rescue ovulation defects of *nmy-1(sb115)* animals. Three animals for each condition, WT, *nmy-1(sb115),* and *nmy-1(sb115),* expressing spermatheca specific GFP::NMY-1, were grown at 20^{o}C on individual NGM plates and live offspring produced per animal were counted and subsequently removed from days 1-7 of adulthood. GFP::NMY-1 is able to rescue spermathecal contractility and ovulation defects indicating GFP::NMY-1 is functional. We observed normal ovulations in young adult animals, however, these animals still produce significantly fewer live offspring than WT, possibly from a combination of ovulation defects in older adults and embryonic elongation defects. This may be due to the fact that GFP::NMY-1 is not under its endogenous promoter, but rather the *fln-1*promoter,which does not fully recapitulate *nmy-1* expression patterns.Error bars represent SEM. Unpaired t test P value: ns P > 0.05,*** P ≤ 0.001,**** P ≤ 0.0001.

Supplemental Figure 2: *De novo* actin polymerization contributes to spermathecal actin network maturation. (A-F) Confocal maximum intensity projections of excised and stained spermathecae from animals before (A-C) and after (D-F) the first ovulation. A and D show F-actin stained with phalloidin (red), B and E show G-actin stained with Deoxyribonuclease I (DNase I; green), and C and F are the merged images. (G) Quantification of phalloidin and DNaseI fluorescence intensity of individual cells for each condition. Phalloidin and DNaseI measurements from the same cell are linked with a black line. For pre-ovulation animals n = 113 cells and n = 59 cells for post-ovulation animals. No more than three cells were measured from the same animal. (H) Quantification of the ratio of F-actin fluorescence intensity (phalloidin) to G-actin fluorescenceintensity (DNaseI) for each cell shown in G. There is a slight but significant increase in the ratio of F-actin/G-actin in cells from spermathecae after the first ovulation. The L1 arrest procedure described in the methods section was used to generate an age synchronized population of animals with individuals just before and after the first ovulation. L1 larvae were prepared and grown on NGM seeded with OP50 *Escherichia coli*for 40 hours at 23°C. Animals were dissected, fixed, stained, rinsed and mounted as described in the methods section except that a 1 hour blocking step in 1% BSA PBST (PBS and 0.05% Triton- X) at

room temperature was added prior to staining and dissected animals were stained for 1 hour at room temperature with constant mixing in blocking buffer with Texas Red-X phalloidin (Invitrogen, Carlsbad, CA, USA; final concentration 0.165 Mm) and DNaseI (Waltham, MA USA ;final concentration 0.3 µM). Scale bar: 20 µm.Error bars represent SEM. Unpaired t test P value:** P ≤ 0.01.

Supplemental Figure 3: Three *In vivo* actin markers produce similar results and recapitulate F-actin organization observed with phalloidin staining. Each image is a confocal maximum intensity projection from a 4-D ovulation movie at the indicated time intervals.In line UN1502 actin is labeled with GFP (GFP::ACT-1) and in UN1612 actin is labeled by expression of the actin binding utrophincalponin homology domain fused with GFP (GFP::UtrCH). In both lines, actin is shown in green. In line UN1654 actin is labeled by expression of the actin binding domain from moesin fused with mCherry (moeABD::mCherry) and myosin is labeled with GFP (GFP::NMY-1). In UN1654 actin is shown in red and myosin in green. Oocyte dwell time is frequently extended in line UN1502 by failure of the valve to open completely when illuminated with the 488 nm laser during image acquisition (see 750 sec time point and Supplemental Movie 2). This was rarely seen when line UN1502 was illuminated only after the valve started to open and was almost never observed in other lines. The slightly more rapid oocyte transit in line UN1654 compared to UN1612 may be due to the increased expression of myosin (GFP::NMY-1). Scale bar: 20µm.

Supplemental Figure 4: Knock down of myosin phosphatase, *mel-11*, produceshypercontractilespermathecae capable of contracting without oocyte entry.Confocal maximum intensity projections of spermathecae expressing INX-12::mApple to label lateral junctions (red) stained with phalloidin to label F-actin (green). The brightfield image is a central sagittal z-slice showing a cross section of the spermatheca with basal actin bundles (green), lateral junctions (red), and brightfield (grayscale). Sperm and oocytes are false colored in blue and pink, respectively. Scale bar: 20µm. (Left panel) Before the first ovulation, in both WT and *mel-11(RNAi)*spermathecae, cells are compact and basal actin bundles are tortuous, interconnected, and misaligned with respect to the long axis of the cell. (Middle panel) Oocyte entry in both WT and *mel-11(RNAi)*spermathecae triggers contraction driving production of prominent actin bundles. In WT cells actin bundles are parallel and regularly spaced. In *mel-11(RNAi)* cells large actin bundles with increased spacing between bundles are apparent. (Right panel) *mel-11(RNAi)*spermathecae appear hypercontractile and are capable of contracting without oocyte entry. Instead, contraction is triggered by a small amount of sperm entering the spermatheca. This was not observed for WT spermathecae. Contraction of a relatively empty spermatheca results in compaction of cells and the actin cytoskeleton (white arrowheads). This obscures actin structures making it difficult to determine the contribution of cell stretch to actin organization other than the requirement of stretch to trigger contraction in WT cells.

Supplemental Figure 5: Altered myosin activity produces similar results in two different *in vivo* actin marker lines. (A-B) Confocal maximum intensity projections of spermathecae expressing actin labeled with GFP, GFP::ACT-1(A), and GFP fused with the actin binding calponin homology domain of utrophin, GFP::UtrCH (B). In both lines, loss of nonmuscle myosin II either my RNAiknockdown, nmy-1(RNAi), or the null allele, *nmy-1(sb115),* result in flaccid spermathecae with tortuous actin bundles. WT have straight, parallel actin bundles. RNAiknockdown of myosin phosphatase, *mel-11*, produces populations of differently oriented bundles within the same cell.(A'-B') Alignment of bundles is highlighted using OrientationJ to false color actin bundles according to their orientation. Selected cells are indicated by yellow boxes in A and B. Scale bar: 20 µm (A-B) and 5 µm (A'-B').

Supplemental Figure 6: Myosin activity influences periodicity and prominence of actin bundles**.** Representative line scan analysis data using *in vivo* actin marker line UN1502 expressing GFP labeled actin, GFP::ACT-1 (A), and N2 stained with phalloidin to label F-actin (B). Both methods for visualizing F-actin produce similar results. Changes in actin bundle prominence and spacing were assessed by measuring the fluorescence intensity along a line drawn across the center of each cell (shown in yellow to the left of each graph). WT cells have actin bundles with regular fluorescence intensity and periodicity seen in the regular height and spacing of peaks (green circles on graphs). Cells depleted of nonmuscle myosin II, *nmy-1(RNAi)* cells*,*have few prominent actin bundles and produce fewer peaks than WT. Additionally, line scans of *nmy-1(RNAi)* cells produce peaks that are not much higher than neighboring valleys (red squares on graphs). Cells depleted of myosin phosphatase, *mel-1(RNAi)*cells*,* have the opposite phenotype and produce populations of bundles that are more prominentthan WT. Line scan analysis of *mel-11(RNAi)* cells produces peaks are brighter than peaks in WT and these bright peaks are spaced further apart, suggesting prominent bundles result from neighboring bundles being pulled together.Scale bar: 5 µm (A'-B').

Supplemental Figure 7: Myosin activity influences periodicity and prominence of actin bundles. Quantification of line scan analysis using GFP labeled actin, GFP::ACT-1 (A-C), and phalloidin (D-F)to visualize F-actin in wild-type cells (WT), and cells treated with RNAi against nonmuscle myosin II (*nmy-1(RNAi)*cells)*,* and RNAi against myosin phosphatase (*mel-11(RNAi)* cells). Both techniques for visualizing actin produce similar trends. (A and D)Measurements of the distance between individual peaks are shown. Cells treated with RNAi against *mel-11* produce populations of peaks that are spaced further apart than peaks measured in WT or *nmy-1(RNAi)* cells. (B and E)Measurements of peak prominence (height above nearest valley) are shown for individual peaks. Knockdown of *nmy-1* reduces peak prominence compared to WT and knockdown of me*l-11* increases peak prominence of a subpopulation of bundles measured. (C and F)Quantification of the number of peaks counted in individual cells shows that both *nmy-1(RNAi)* and *mel-11(RNAi*) cells have fewer peaks than WT. In *nmy-1(RNAi)* cells this is because few bright actin bundles are produced. In *mel-11(RNAi)* cells this is because the spacing between prominent peaks is increased such that an individual cell contains fewer bundles than WT, but these bundles are brighter. In A-C bundles from 10 cells were measured for each

condition, and n = 111, 65, and 83 individual bundles for WT, *nmy-1(RNAi)*, and *mel-11(RNAi),* respectively. In D-E bundles from 6 to 8 cells were measured for each condition,and n = 72, 31, and 38 individual bundles for WT, *nmy-1(RNAi)*, and *mel-11(RNAi),* respectively. No more than 2 cells were measured from the same animal. Unpaired t test with (A-B and D-E) or without (C and F) Welch's correction P value * ≤ 0.05, ** ≤ 0.01, *** P ≤ 0.001, **** P ≤ 0.0001. Scale bar = 5 μm.

Supplemental Figure 8: RNAi depletion of nonmuscle myosin II, *nmy-1*, or myosin phosphatase, *mel-11*, does not alter pre-ovulation basal actin bundle organization.Confocal maximum intensity projections of excised spermathecae before the first ovulation from wild-type animals (WT) and animals treated with RNAi against nonmuscle myosin II (*nmy-1(RNAi)*)and myosin phosphatase (*mel-11(RNAi)*) stained with phalloidin to label F-actin. White boxes indicate section magnified in inserts to the right. All inserts are a single confocal z-slice showing only the most basal surface. Yellow line outlines an individual cell. Note the similar tortuous basal actin bundles in all conditions. The only striking difference between wild-type and RNAi treated spermathecae is the distended, disorganized valve in *nmy-1(RNAi)*spermathecae. The valve in each image is indicated by white brackets. Scale bar: 20 μm, 5 μm (inserts).

Supplemental Figure 9: Elevated myosin activity alters myosin distribution within actomyosin bundles producing myosin clusters that grow by fusion of clusters along a single actin bundle**.** **(**A)Kymographs from four different confocal 4-D ovulation movies in animals, expressing moeABD::mCherry to label actin (red) and GFP::NMY-1 to label myosin (green), treated with RNAi against myosin phosphatase, *mel-11*. Kymographs were generated from maximum intensity projections of ovulation movies. A vertical line with a pixel width of 40 was drawn down the center of each cell and the fluorescence intensity along this line was measured for 51 frames spanning 17 min beginning at oocyte entry. Immediately after oocyte entry (left side of kymographs), actin and myosin fluorescence is homogenously distributed. By ~5 min after oocyte entry,horizontal bands of increased actin and myosin fluorescence intensity are apparent. These bands increase in fluorescence intensity and grow by fusion (see white arrow heads in movies 2 and 4). (B) Fluorescence intensity of myosin clusters increases between 5 and 20 min after oocyte entry. Each point represents a single myosin clusters measured within 1-3 cells from each movie. (C) The distance between myosin clusters increases as smaller clusters fuse together between 5 and 20 min after oocyte entry. Each point represents the distance between two clusters along a single bundle within 1-3 cells from each movie.In B-C, n = 40, 21, 31, and 28 myosin clusters at 5 min and n = 56, 48, 90, and 31 myosin clusters at 20 min for movies 1-4, respectively. Error bars represent SEM. Unpaired t test P value ns P > 0.05, * ≤ 0.05, ** ≤ 0.01, *** P ≤ 0.001, **** P ≤ 0.0001. Horizontal scale bar: 5 min, vertical scale bar: 5 μm.

Supplemental Table 1: *C. elegans*strains

Strain Name	Genotype
UN1502	*xbIs1502[fln-1p::GFP::act-1, rol-6]*
UN1514	*xbIs1404[fln-1p::inx-12::mApple]*
UN1534	*xbIs1502[fln-1p::GFP::act-1, rol-6]; plc-1(rx1)*
UN1537	*xbIs1527[fln-1p::GFP::nmy-1, rol-6]*
UN1612	*xbIs1612[fln-1p::GFP::UtrCH, rol-6, ttx3p::RFP]*
UN1654	*xbIs1527[fln-1p::GFP::nmy-1, rol-6]; qyIs198[inft-1p::moeABD::mCherry, unc-119(+)]; unc-119(ed4)*
UN1655	*xbIs1527[fln-1p::GFP::nmy-1, rol-6]; nmy-1(sb115)*

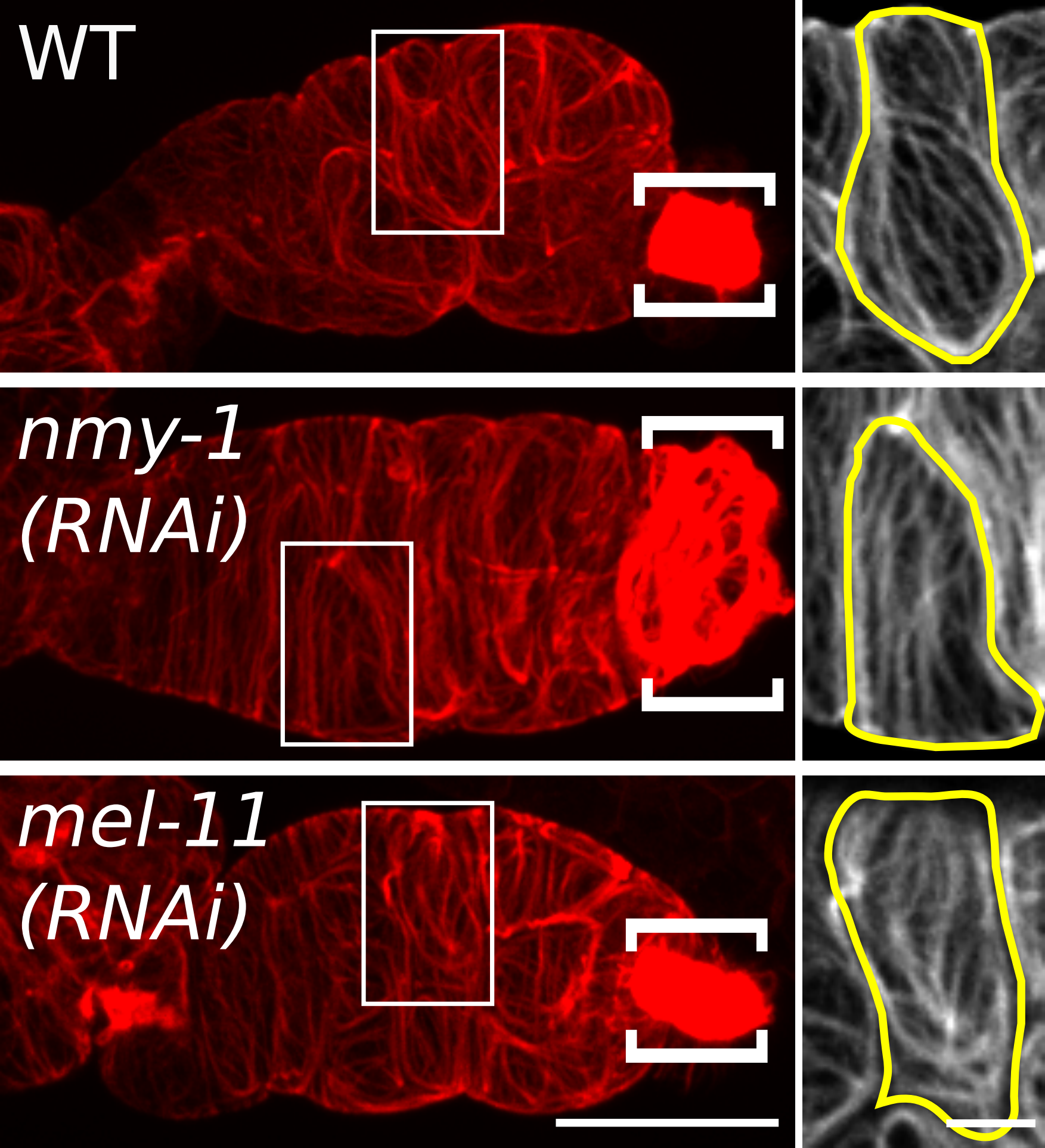
WT
nmy-1
(RNAi)
mel-11
(RNAi)

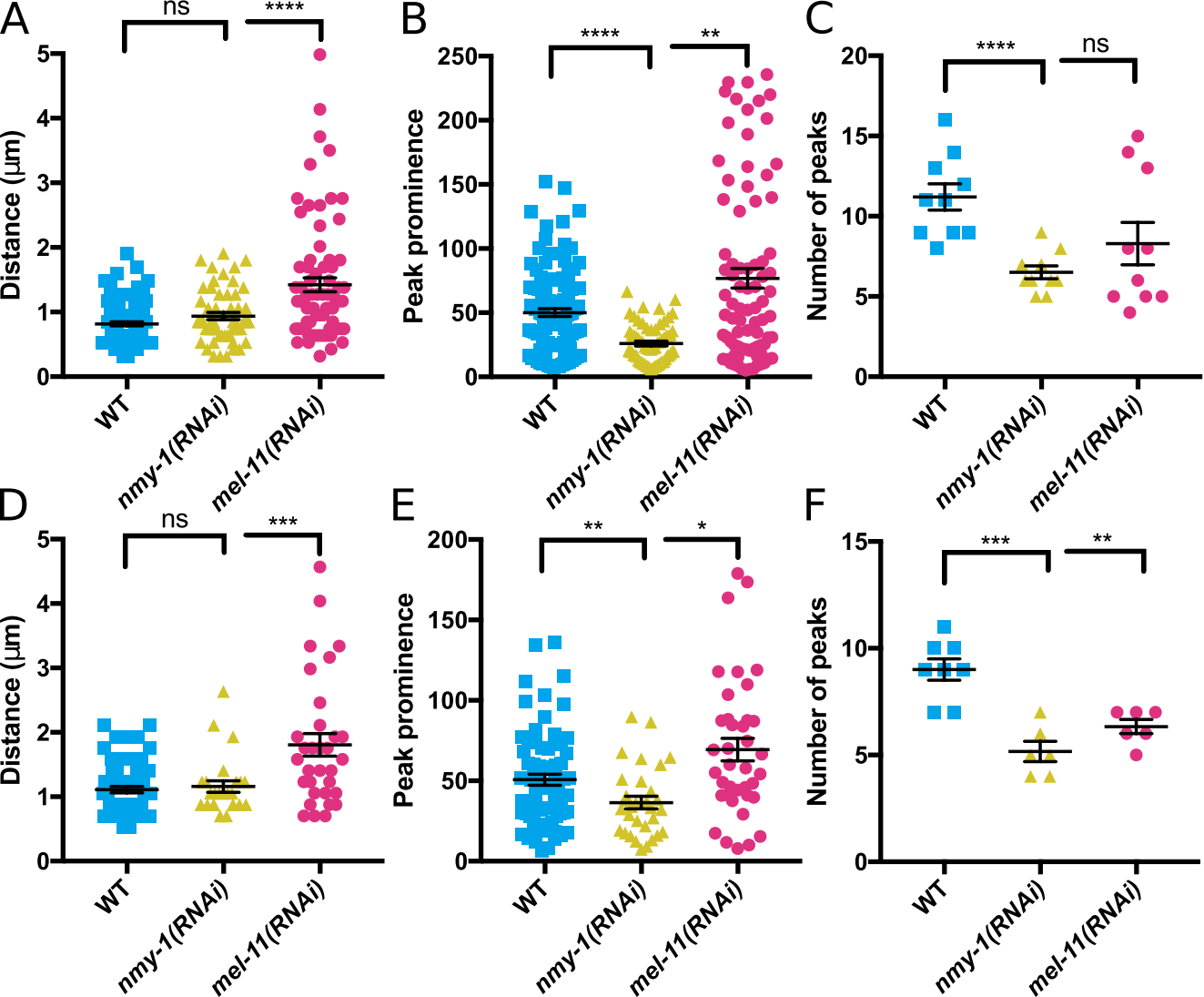
A
Distance (µm)
ns
****
WT
nmy-1(RNAi)
mel-11(RNAi)
B
Peak prominence
****
**
C
Number of peaks
****
ns
D
Distance (µm)
ns
***
E
Peak prominence
**
*
F
Number of peaks
***
**

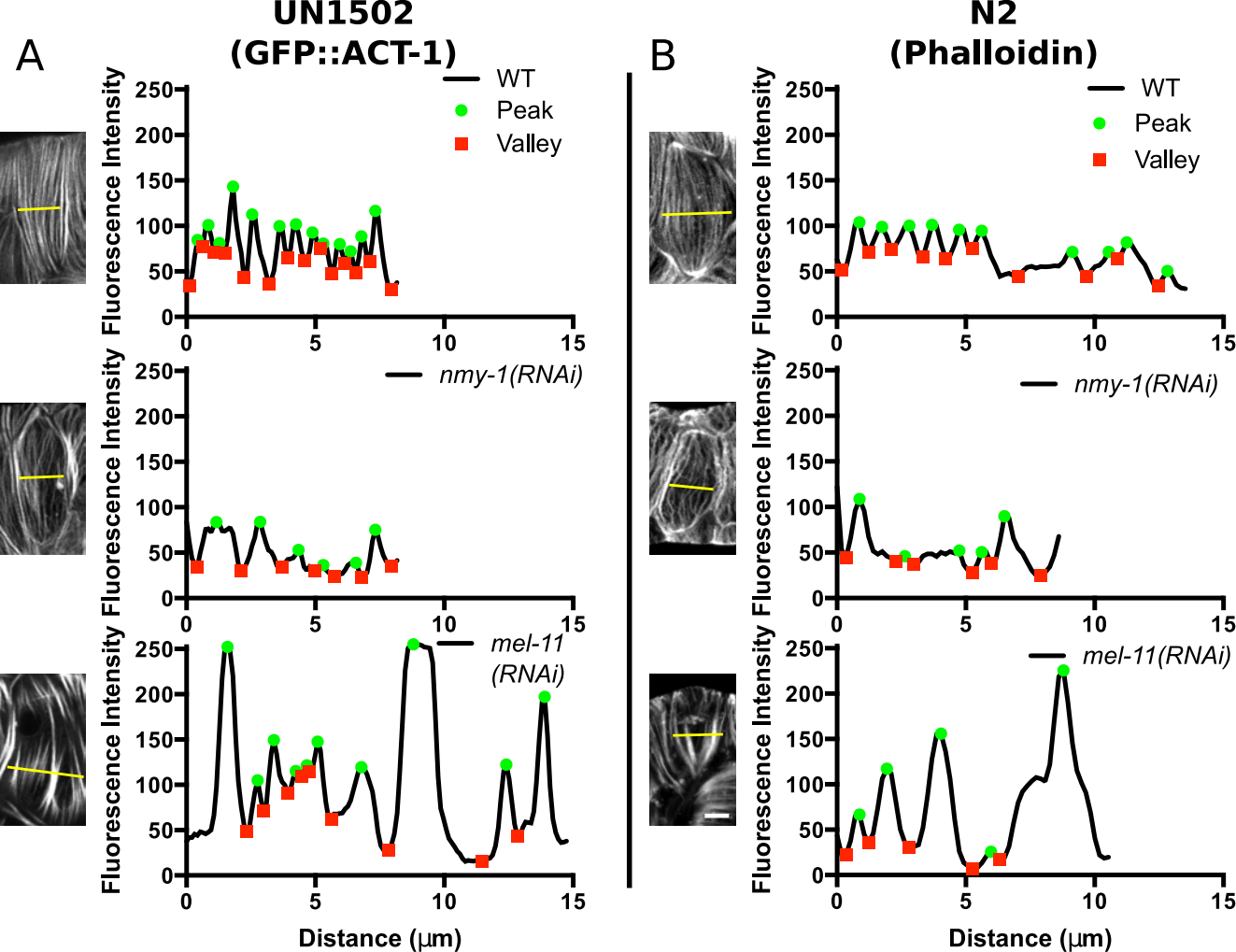
A
UN1502
(GFP::ACT-1)
B
N2
(Phalloidin)
WT
Peak
Valley
nmy-1(RNAi)
mel-11
(RNAi)
mel-11(RNAi)
Fluorescence Intensity
Distance (μm)
0
5
10
15
50
100
150
200
250

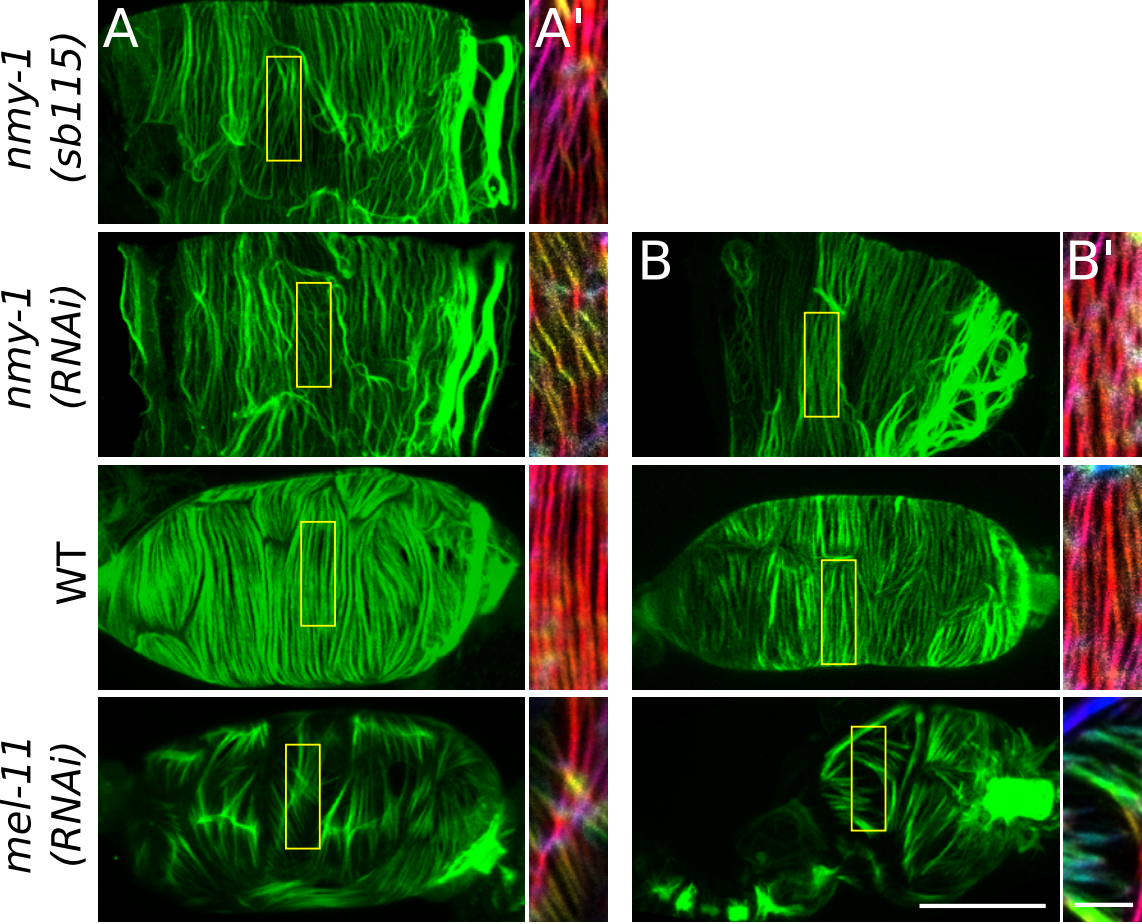
A
A'
B
B'
nmy-1 (sb115)
nmy-1 (RNAi)
WT
mel-11 (RNAi)
UN1502 (GFP::ACT-1)
UN1612 (GFP::UtrCH)

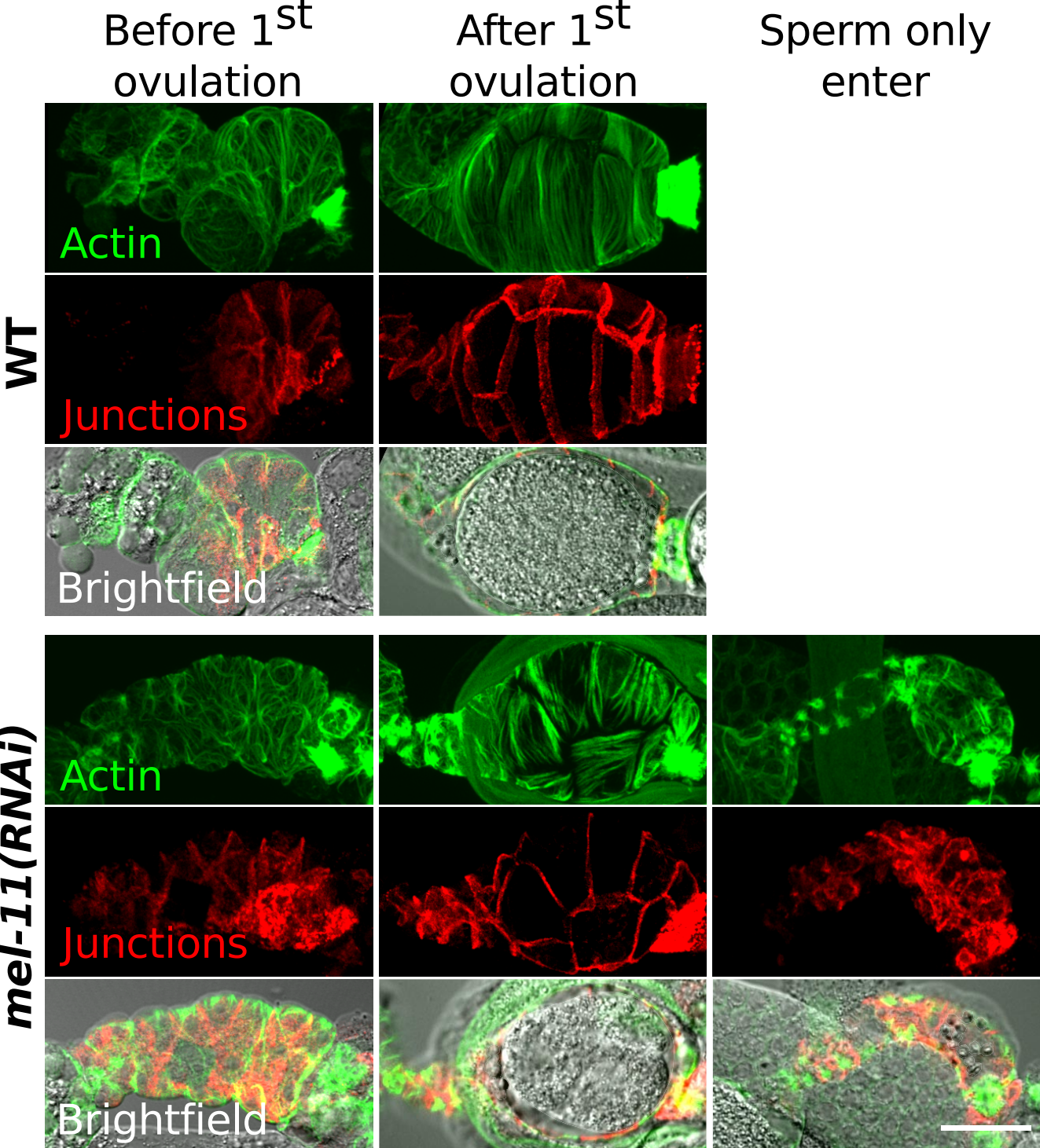
Before 1st ovulation
After 1st ovulation
Sperm only enter
WT
mel-11(RNAi)
Actin
Junctions
Brightfield
Actin
Junctions
Brightfield

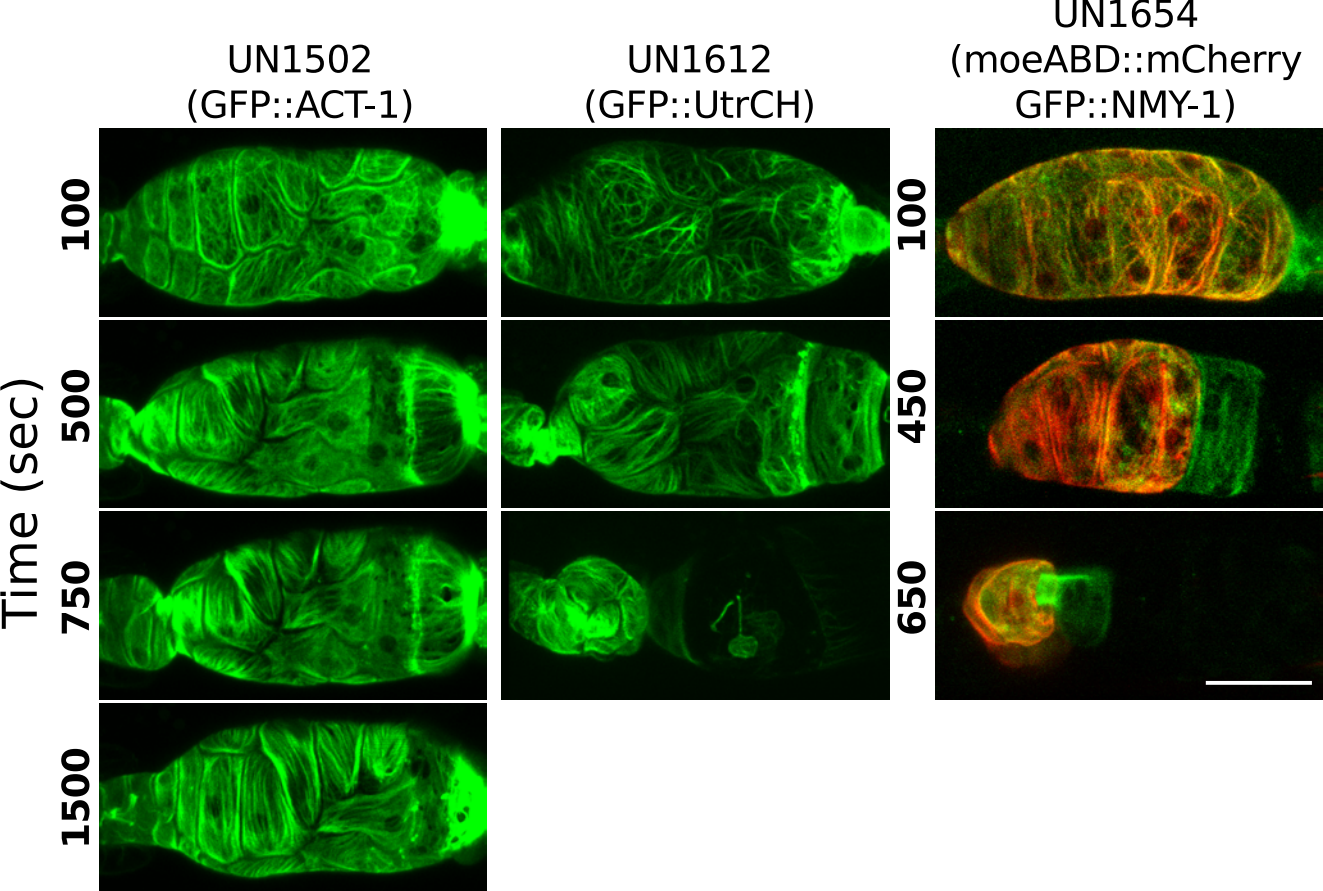
UN1502
(GFP::ACT-1)
UN1612
(GFP::UtrCH)
UN1654
(moeABD::mCherry
GFP::NMY-1)
Time (sec)
100
500
750
1500
100
450
650

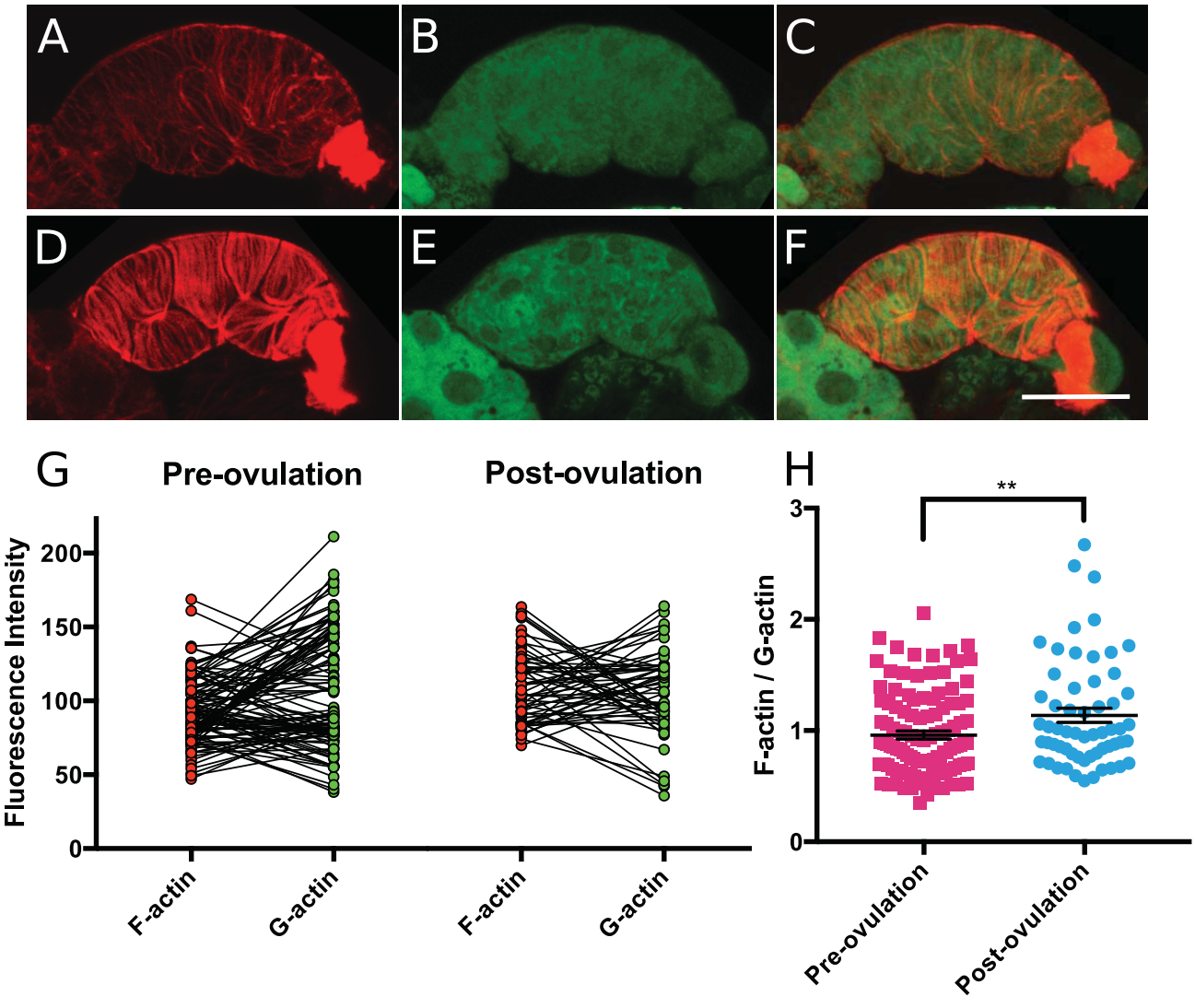
A
B
C
D
E
F
G
Pre-ovulation
Post-ovulation
Fluorescence Intensity
200
150
100
50
0
F-actin
G-actin
F-actin
G-actin
H
**
F-actin / G-actin
3
2
1
0
Pre-ovulation
Post-ovulation

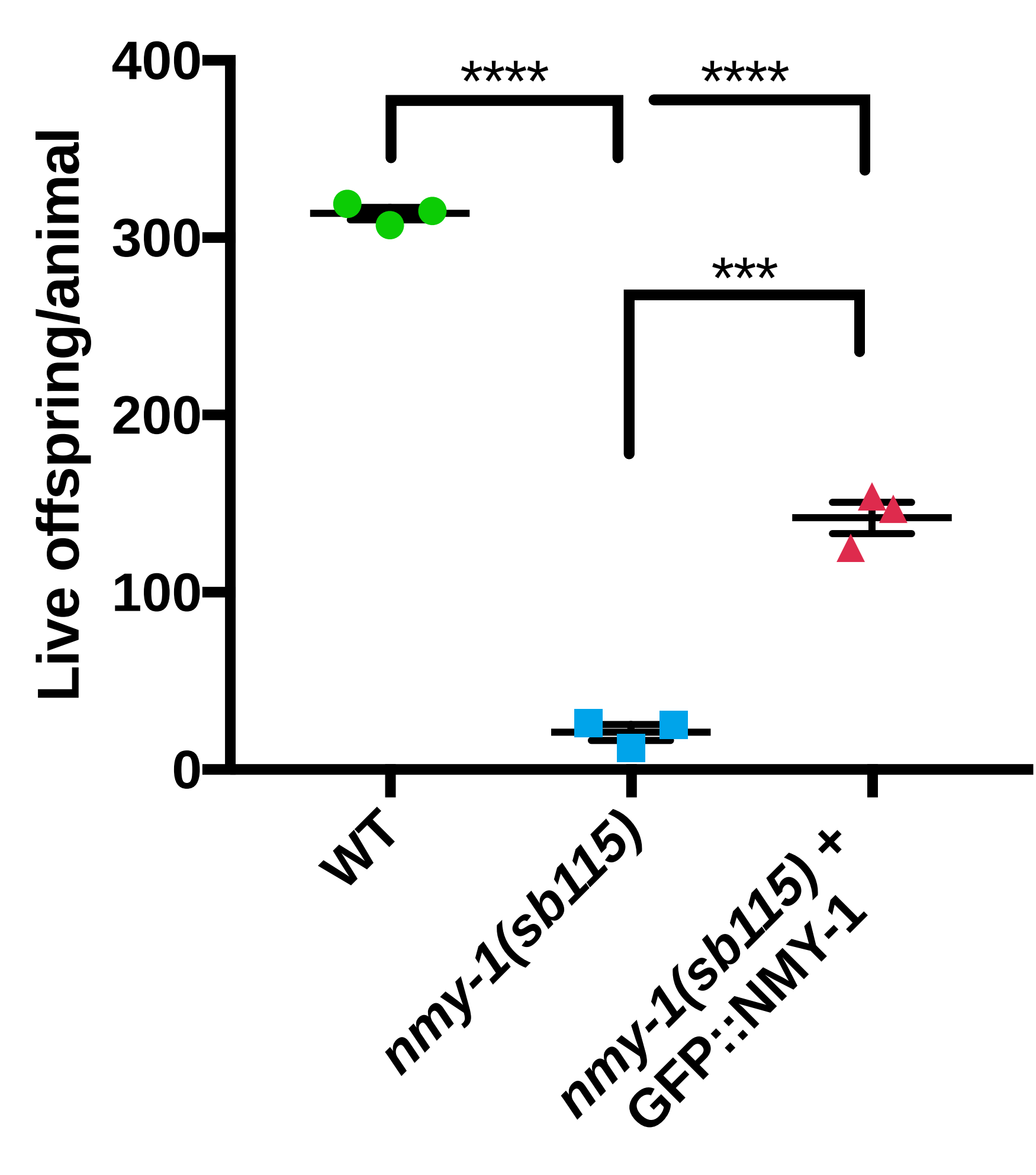
Live offspring/animal
400
300
200
100
0
****
****
***
WT
nmy-1(sb115)
nmy-1(sb115) + GFP::NMY-1

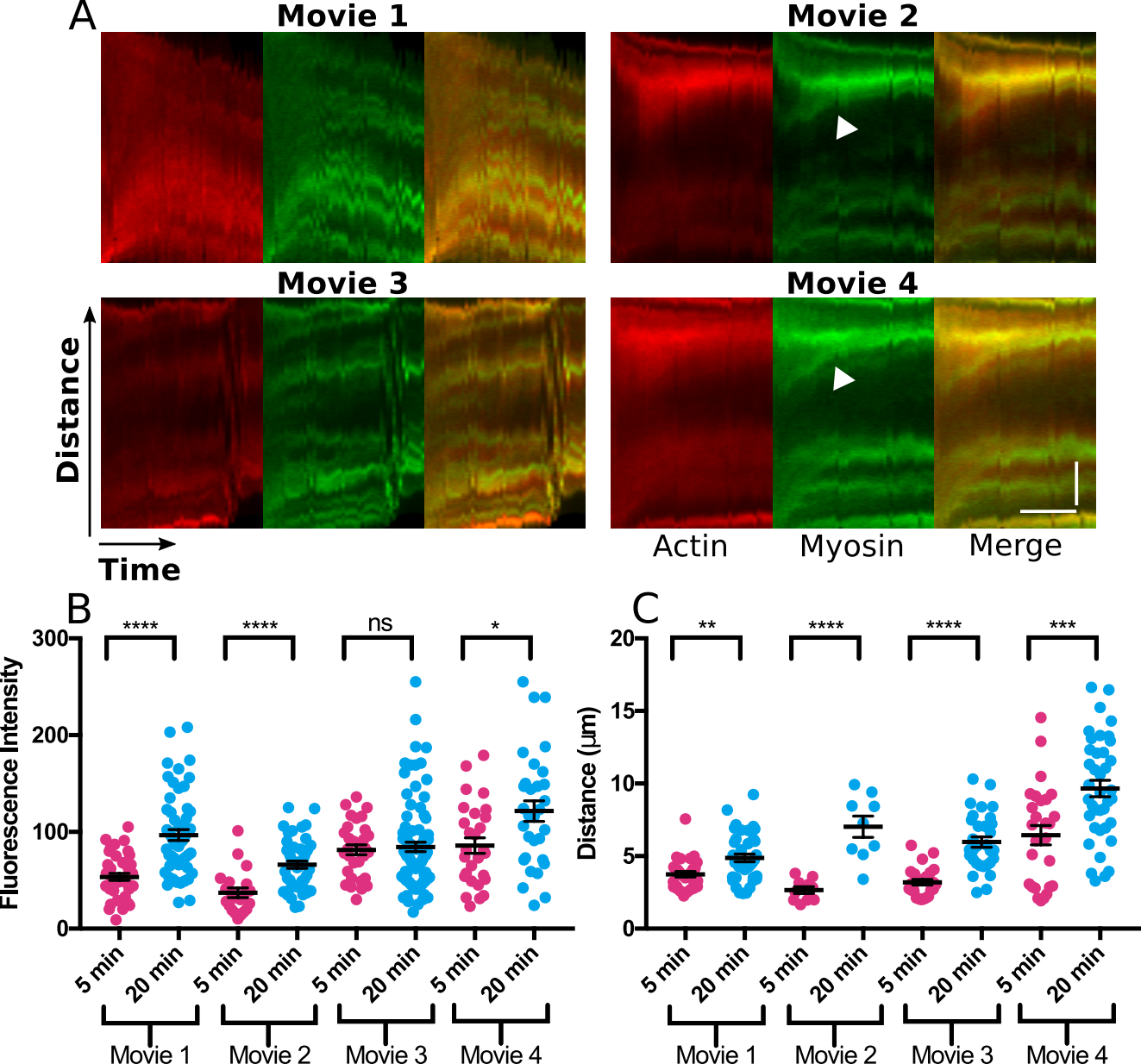
A
Movie 1
Movie 2
Movie 3
Movie 4
Distance
Time
Actin
Myosin
Merge
B
Fluorescence Intensity
300
200
100
0
****
****
ns
*
5 min
20 min
Movie 1
Movie 2
Movie 3
Movie 4
C
Distance (µm)
20
15
10
5
0
**
****
****
***

Supplemental Figure 9: Elevated myosin activity alters myosin distribution within actomyosin bundles producing myosin clusters that grow by fusion of clusters along a single actin bundle. (A) Kymographs from four different confocal 4-D ovulation movies in animals, expressing moeABD::mCherry to label actin (red) and GFP::NMY-1 to label myosin (green), treated with RNAi against myosin phosphatase, mel-11. Kymographs were generated from maximum intensity projections of ovulation movies. A vertical line with a pixel width of 40 was drawn down the center of each cell and the fluorescence intensity along this line was measured for 51 frames spanning 17 min beginning at oocyte entry. Immediately after oocyte entry (left side of kymographs), actin and myosin fluorescence is homogenously distributed. By ~5 min after oocyte entry, horizontal bands of increased actin and myosin fluorescence intensity are apparent. These bands increase in fluorescence intensity and grow by fusion (see white arrow heads in movies 2 and 4). (B) Fluorescence intensity of myosin clusters increases between 5 and 20 min after oocyte entry. Each point represents a single myosin clusters measured within 1-3 cells from each movie. (C) The distance between myosin clusters increases as smaller clusters fuse together between 5 and 20 min after oocyte entry. Each point represents the distance between two clusters along a single bundle within 1-3 cells from each movie. In B-C, n = 40, 21, 31, and 28 myosin clusters at 5 min and n = 56, 48, 90, and 31 myosin clusters at 20 min for movies 1-4, respectively. Error bars represent SEM. Unpaired t test P value ns $P > 0.05$, * ≤ 0.05, ** ≤ 0.01, *** $P \leq 0.001$, **** $P \leq 0.0001$. Horizontal scale bar: 5 min, vertical scale bar: 5 µm.